Int. J. Heat Mass Transfer. Vol. 24, pp. 323 333
Pergamon Press Ltd. 1981. Printed in Great Britain

0017-9310/81/0201-0323 $02.00/0

ANALYSIS OF HEAT TRANSFER DURING HYDRAIR COOLING OF SPHERICAL FOOD PRODUCTS

P. M. ABDUL MAJEED
Department of Mechanical Engineering, Regional Engineering College,
Calicut, Kerala, 673 601, India

(*Received* 14 *November* 1979 *and in revised form* 25 *July* 1980)

Abstract — Hydrair cooling of perishable food products is expected to incorporate the advantages of both air cooling and hydrocooling processes. This technique consists of passing cold air over a product which is continuously wetted by a spray of chilled water. An analysis which yields the time–temperature histories during hydrair cooling of spherical food products is presented. The ranges of parameters in which the process is most effective are identified. The cooling speed and the governing parameters are correlated.

NOMENCLATURE

a, half thickness of product [m];
$A_0, A_1, \ldots$, coefficients of equation (11);
Bi, Biot number;
C_p, specific heat of dry air [kJ/kg K^{-1}];
C_{pw}, specific heat of water vapour [kJ/kg K^{-1}];
d, coordinate distance from surface along diameter [m];
g, acceleration due to gravity [m/h^2];
h, convective heat-transfer coefficient [kJ/h m^2 K^{-1}];
H, specific enthalpy of moist air [kJ/kg];
$I_1, I_2, \ldots$, coefficients of equation (23);
$J_1, J_2, \ldots$, coefficients of equation (32);
k, thermal conductivity [kJ/h m^{-1} K^{-1}];
Q, film flow rate per wetted perimeter [m^2/h];
r, radial coordinate [m];
R, radius of sphere [m];
Re, Reynolds number;
R_T, temperature ratio defined in equation (19);
t, time [h];
T, temperature [K];
v_ϕ, velocity of film flow [m/h];
W, humidity ratio [kg moisture/kg dry air];
x, y, coordinate distance [m];
Z, half-cooling time of dimensionless time t^*.

Greek symbols

α, thermal diffusivity [m^2/h];
δ, film thickness [m];
ν, kinematic viscosity [m^2/h].

Subscripts

0, initial condition;
a, air wet bulb;
f, water film;
if, product–water interface;
m, at $\phi = \pi/2$;
p, product;
s, air–water interface.

Superscripts

*, non-dimensional quantity defined in equation (19);
+, non-dimensional independent parameter defined in equation (43).

INTRODUCTION

HYDRAIR cooling is a new technique of food cooling which combines the advantages of the conventional air cooling and hydrocooling. The process which consists of passing cold air over the product continuously wetted by a spray of chilled water, is under preliminary stages of investigation. Hydrair cooling has been experimentally studied by some investigators [1–3] and under certain operating conditions, has been reported to be even better than hydrocooling where cooling is effected by maintaining a flow of chilled water past the product. An analytical study leading to the prediction of the cooling performance during hydrair cooling of a slab-shaped food product is presented by Abdul Majeed [4].

This paper presents the results of a theoretical analysis of the problem of hydrair cooling in the case of a spherical food product. The energy equations for the product and the water film are solved using the finite difference technique. The results are obtained in terms of dimensionless parameters covering the product properties and processing conditions encountered in food cooling practice.

THEORETICAL ANALYSIS

Description of the physical model

The physical model used for the analysis of the problem is represented in Fig. 1(a). The product, having an initial temperature of T_{p0}, is continuously

wetted by a film of water having an initial temperature of T_{f0}. Cold air with a wet bulb temperature T_a flows over the wetted product yielding a uniform surface heat-transfer coefficient, h. The product has a radius R. The thickness of the liquid film varies over the product but is symmetrical with respect to the vertical axis. Heat and mass transfer takes place from the liquid film into the stream of cold air.

Formulation of the problem

The coordinate system for the analysis is shown in Fig. 1. The film temperature varies with ϕ and r but is invariant in the ψ (azimuthal angle) direction because of the symmetry of flow and heat-transfer conditions in that direction. Application of the continuity, momentum and energy equations to the layer of flowing liquid results in the governing equation of the form,

$$\alpha_f\left(\frac{\partial^2_{T_f}}{\partial r^2}+\frac{2}{r}\frac{\partial T_f}{\partial r}\right)-\frac{v_\phi}{r}\frac{\partial T_f}{\partial \phi}=\frac{\partial T_f}{\partial t} \tag{1}$$

where v_ϕ denotes the velocity at any point r in the liquid film. For smooth laminar two dimensional flow over a vertical surface, v_ϕ is given by [5]

$$v_\phi=\frac{g}{\nu_f}\sin\phi(\delta y_f-y_f^2/2) \tag{2}$$

where y_f is the distance from the surface to any point in the film defined as

$$y_f=r-R. \tag{3}$$

Due to the heat transfer in the film being two-dimensional, the heat transfer within the product also is two-dimensional which is written as,

$$\frac{\partial^2 T_p}{\partial r^2}+\frac{2}{r}\frac{\partial T_p}{\partial r}+\frac{\cot\phi}{r^2}\frac{\partial T_p}{\partial \phi}+\frac{1}{r^2}\frac{\partial^2 T_p}{\partial \phi^2}=\frac{1}{\alpha_p}\frac{\partial T_p}{\partial t}. \tag{4}$$

The two boundary conditions in the r-direction are identified from energy balance considerations at the product–liquid film interface on diametrically opposite points. To facilitate using these conditions, the origin of the coordinate system is shifted from the centre to the periphery and the (r,ϕ) system changed to (d,θ) system as shown in Fig. 1(b) and 1(c) by the following transformations.

(a) For the region $d=0$ to R and $\theta=0$ to π

$$r=(R-d) \quad \text{and} \quad \phi=(\theta+\pi) \tag{5}$$

(b) For the region $d=R$ to $2R$ and $\theta=0$ to π

$$r=(d-R) \quad \text{and} \quad \phi=\theta. \tag{6}$$

Introduction of substitution given by equations (5) or (6) into equation (4) will yield the same equation given by,

$$\frac{\partial^2 T_p}{\partial d^2}+\frac{2}{(d-R)}\frac{\partial T_p}{\partial d}+\frac{\cot\theta}{(d-R)^2}\frac{\partial T_p}{\partial \theta}+\frac{1}{(d-R)^2}\frac{\partial^2 T_p}{\partial \theta^2}=\frac{1}{\alpha_p}\frac{\partial T_p}{\partial t}. \tag{7}$$

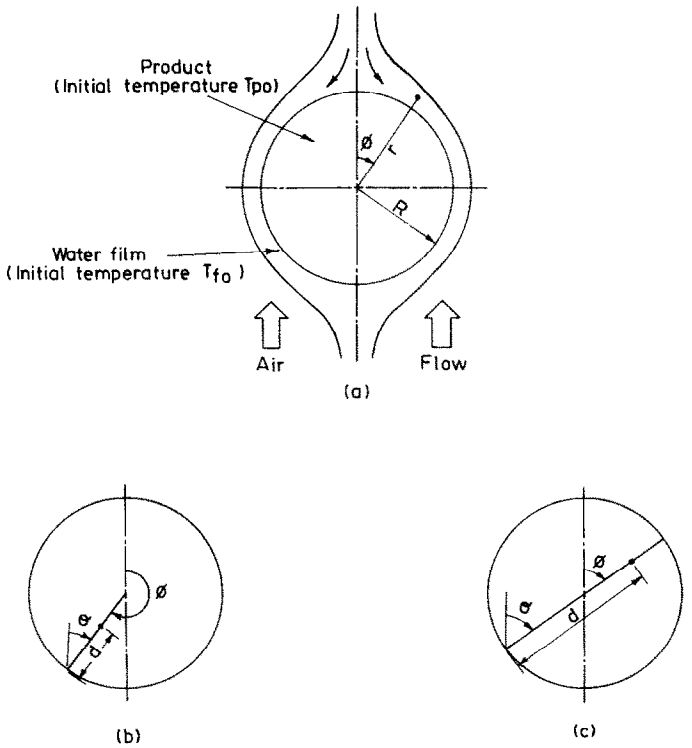

FIG. 1. Physical model and coordinate system.

The initial and boundary conditions of equation (1) are obtained as follows:

The initial uniform temperature within the liquid film yields:

$$T_f = T_{f0} \quad \text{at } t = 0 \quad \text{for } R \le r \le (R + \delta) \quad \text{and } 0 \le \phi \le 2\pi. \quad (8)$$

A continuous flow of water is assumed from the top of the product to maintain a film of flowing water. This gives the condition,

$$T_f = T_{f0} \quad \text{at } \phi = 0 \quad \text{for } R < r \le (R + \delta) \quad \text{and } t \ge 0. \quad (9)$$

At the surface of the water film the energy exchange with the air stream takes place by a combination of sensible and latent heat transfer. This is taken into account using the definition of enthalpy potential [6] which when applied to the liquid film yields,

$$-k_f \frac{\partial T_f}{\partial r} = \frac{h}{C_p + WC_{pw}}(H_s - H_a) \quad \text{at } r = (R + \delta) \quad \text{for } 0 < \phi \le 2\pi \quad \text{and } t > 0 \quad (10)$$

where H_a is the specific enthalpy of the free stream air which is generally unsaturated. The enthalpy of unsaturated air can be represented with sufficient accuracy by the enthalpy of saturated air at its thermodynamic wet bulb temperature [7]. The enthalpy of saturated air can be expressed as a function of the temperature by a second degree polynomial as,

$$H = A_0 + A_1 T + A_2 T^2. \quad (11)$$

At the product–water interface, a good thermal contact between the two is assumed to exist resulting in the same temperature for both product and water film. Thus,

$$T_p = T_{if}(\phi, t) \quad \text{at } d = 0 \quad \text{and } d = 2R \quad \text{for } 0 \le \theta \le \pi \quad \text{and } t > 0 \quad (12)$$

$$T_f = T_{if}(\phi, t) \quad \text{at } r = R \quad \text{for } 0 \le \phi \le 2\pi \quad \text{and } t > 0. \quad (13)$$

Equations (1), (8)–(10) and (13) completely define the problem of heat conduction in the liquid film.

For the product, based on the physical model, the following initial and boundary conditions are written for equation (7):

$$T_p = T_{p0} \quad \text{at } t = 0 \quad \text{for } 0 \le d \le 2R \quad \text{and } 0 \le \theta \le \pi \quad (14)$$

$$\frac{\partial T_p}{\partial \theta} = 0 \quad \text{at } \theta = 0 \quad \text{for } 0 \le d \le 2R \quad \text{and } t \ge 0 \quad (15)$$

and

$$\frac{\partial T_p}{\partial \theta} = 0 \quad \text{at } \theta = \pi \quad \text{for } 0 \le d \le 2R \quad \text{and } t \ge 0 \quad (16)$$

Energy balance at the interface results in,

$$k_p \frac{\partial T_p}{\partial d} = -k_f \frac{\partial T_f}{\partial r} \quad \text{at } d = 0 \quad \text{for } 0 \le \theta \le \pi \quad \text{and } t > 0 \quad (17)$$

and

$$-k_p \frac{\partial T_p}{\partial d} = -k_f \frac{\partial T_f}{\partial r} \quad \text{at } d = 2R \quad \text{for } 0 \le \theta \le \pi \quad \text{and } t > 0. \quad (18)$$

Equations (7), (14)–(18) completely define the problem of heat conduction within the product.

In order to obtain the results in a generalised form, the governing equations and boundary conditions are non-dimensionalised using the following definitions:

$$d^* = \frac{d}{2R}, \quad r^* = \frac{r - R}{\delta}, \quad T_p^* = \frac{T_p - T_a}{T_{p0} - T_a},$$

$$T_f^* = \frac{T_f - T_a}{T_{f0} - T_a}, \quad T_s^* = \frac{T_s - T_a}{T_{f0} - T_a},$$

$$T_{if}^* = \frac{T_{if} - T_a}{T_{f0} - T_a}, \quad R_T = \frac{T_{f0} - T_a}{T_{p0} - T_a},$$

$$Bi = \frac{hR}{k_p}, \quad k^* = \frac{k_p}{k_f}, \quad \alpha^* = \frac{\alpha_p}{\alpha_f},$$

$$t^* = \frac{\alpha_p t}{R^2}, \quad R^* = \frac{gR^3}{\nu_f^2}, \quad \delta_m^* = \frac{\delta_m}{R},$$

where

$$\delta_m = \delta \quad \text{at } \phi = \frac{\pi}{2}. \quad (19)$$

The dimensionless distance r^* varies from 0 at the product surface to 1 at the film surface. The variation of the film thickness δ with ϕ is given by [5],

$$\delta = \left[\frac{3\nu_f^2}{g \sin \phi} Re_f\right]^{1/3} \quad (20)$$

where Re_f represents the film Reynolds number defined by

$$Re_f = \frac{Q}{\nu_f}. \quad (21)$$

For a constant volume flow rate over the product surface,

$$\delta = R\delta_m^* \operatorname{cosec}^{2/3} \phi. \quad (22)$$

On introduction of equations (11), (19) and (22), the governing equations and boundary conditions take the following dimensionless form:

Product.

$$\frac{\partial^2 T_p^*}{\partial d^{*2}} + I_1(d^*)\frac{\partial T_p^*}{\partial d^*} + I_2(d^*)\frac{\partial^2 T_p^*}{\partial \theta^2} + I_3(d^*, \theta)\frac{\partial T_p^*}{\partial \theta} = 4\frac{\partial T_p^*}{\partial t^*} \quad (23)$$

$$T_p^* = 1 \quad \text{at } t^* = 0 \quad \text{for } 0 \le d^* \le 1 \quad \text{and } 0 \le \theta \le \pi \tag{24}$$

$$\frac{\partial T_p^*}{\partial \theta} = 0 \quad \text{at } \theta = 0 \quad \text{for } 0 \le d^* \le 1 \quad \text{and } t^* \ge 0 \tag{25}$$

$$\frac{\partial T_p^*}{\partial \theta} = 0 \quad \text{at } \theta = \pi \quad \text{for } 0 \le d^* \le 1 \quad \text{and } t^* \ge 0 \tag{26}$$

$$\frac{\partial T_p^*}{\partial d^*} = -2\frac{R_T \sin^{2/3}\phi}{k^*\delta_m^*}\frac{\partial T_f^*}{\partial r^*} \quad \text{at } d^* = 0 \quad \text{for } 0 \le \theta \le \pi \quad \text{and } t^* > 0 \tag{27}$$

$$\frac{\partial T_p^*}{\partial d^*} = 2\frac{R_T}{k^*}\frac{\sin^{2/3}\phi}{\delta_m^*}\frac{\partial T_f^*}{\partial r^*} \text{at } d^* = 1 \quad \text{for } 0 \le \theta \le \pi \quad \text{and } t^* > 0 \tag{28}$$

where

$$I_1(d^*) = \frac{2}{(d^* - 0.5)} \tag{29}$$

$$I_2(d^*) = \frac{1}{(d^* - 0.5)^2} \tag{30}$$

$$I_3(d^*, \theta) = \frac{\cot\theta}{(d^* - 0.5)^2}. \tag{31}$$

Liquid film.

$$J_1(\phi)\frac{\partial^2 T_f^*}{\partial r^{*2}} + J_2(\phi, r^*)\frac{\partial T_f^*}{\partial r^*} - J_3(\phi, r^*)\frac{\partial T_f^*}{\partial \phi} = J_4(\phi)\alpha^*\frac{\partial T_f^*}{\partial t^*} \tag{32}$$

$$T_f^* = 1 \quad \text{at } t^* = 0 \quad \text{for } 0 \le r^* \le 1 \quad \text{and } 0 \le \phi \le 2\pi \tag{33}$$

$$T_f^* = 1 \quad \text{at } \phi = 0 \quad \text{for } 0 < r^* \le 1 \quad \text{and } t^* > 0 \tag{34}$$

$$T_f^* = T_{if}^*(\phi, t^*) \quad \text{at } r^* = 0 \quad \text{for } 0 \le \phi \le 2\pi \quad \text{and } t^* > 0 \tag{35}$$

$$\frac{\partial T_f^*}{\partial r^*} = -\left[\frac{J_5}{J_4(\phi)}T_s^* + \frac{J_6}{J_4(\phi)}T_s^{*2}\right] \quad \text{at } r^* = 1 \quad \text{for } 0 < \phi \le 2\pi \quad \text{and } t^* > 0 \tag{36}$$

where,

$$J_1(\phi) = \sin^2\phi/\delta_m^{*2} \tag{37}$$

$$J_2(\phi, r^*) = \frac{2\sin^2\phi}{\delta_m^*[J_4(\phi) + \delta_m^* r^*]} + \frac{2}{3}Pr_f R^*\frac{\delta_m^{*2} r^{*2}(1 - r^*/2)\cos\phi}{J_4(\phi) + \delta_m^* r^*} \tag{38}$$

$$J_3(\phi, r^*) = Pr_f R^*\frac{\delta_m^{*2} r^*(1 - r^*/2)\sin\phi}{J_4(\phi) + \delta_m^* r^*} \tag{39}$$

$$J_4(\phi) = \sin^{2.3}\phi \tag{40}$$

$$J_5 = k^* Bi\delta_m^*\left(\frac{A_1}{C_p + WC_{pw}} + 2T_a^+\right) \tag{41}$$

$$J_6 = k^* Bi\delta_m^*(T_{f0}^+ - T_a^+). \tag{42}$$

In equations (41) and (42), the non-dimensional temperature parameters T_{f0}^+ and T_a^+ are obtained by defining a new parameter, T^+ as,

$$T^+ = \frac{A_2 T}{C_p + WC_{pw}}. \tag{43}$$

The specific heat of air at constant pressure, C_p is assumed to be constant at 1 kJ/kg K^{-1}. The quantity, WC_{pw} may be assumed constant at 0.021 kJ/kg K^{-1}. The coefficients of equation (11) for the range of wet bulb temperatures from -10 to $+10$°C are:

$$A_0 = 9.30770, \quad A_1 = 1.75289, \quad A_2 = 0.02193 \tag{44}$$

which yield H in kJ/kg.

From equations (19), (20) and (22),

$$\delta_m^* = [3Re_m/R^*]^{1/3} \tag{45}$$

where

$$Re_m = Re_f \quad \text{at } \phi = \pi/2. \tag{46}$$

The values of the parameters required for computation are those of k^*, α^*, R^*, T_a^+, T_{f0}^+, T_{p0}^+, Re_m, Pr_f and Bi.

METHOD OF SOLUTION

The solution of the energy equation for the product and the film given respectively by equation (23) and equation (32) is obtained numerically using the finite difference technique. ADI method is used for the solution of equation (23). The equations are solved simultaneously by an iteration procedure described hereunder.

At a time step, a value is assumed for T_{if}^* at every ϕ in equation (35) to solve the energy equation of the film. $\partial T_f^*/\partial r^*$ at $r^* = 0$ for all values of ϕ are calculated from which $\partial T_f^*/\partial r^*$ at $d^* = 0$ and $d^* = 1$ are determined for $0 \le \theta \le \pi$. These are used in equations (27) and (28) and energy equation for product is solved. The values of T_p^* so obtained at $d^* = 0$ and $d^* = 1$ for various values of ϕ are compared with the values corresponding to those assumed for interface temperature T_{if}^* in equation (35). If they are different, another set of values are assumed for T_{if}^* in equation (35) and the procedure is repeated. This is continued till the assumed values of interface temperature and those obtained from the solution of equation (23) agree within allowable tolerance. In the actual computation, an arbitrary uniform value, say 1.2, is

assumed for T_{if}^* at every ϕ in equation (35) and following the above procedure, a set of values of T_p^* at the product surface are calculated. Another arbitrary uniform value, say 1.5, is assumed for T_{if}^* in equation (35) and a second set of calculated values of T_p^* are obtained at the product surface. From the two sets of assumed and calculated values, a third set of values of T_{if}^* is determined by the use of an iteration scheme. This new set of values of T_{if}^* is used to calculate a new set of T_p^* at the product surface and the corresponding values of T_{if}^* and T_p^* are compared at every point. If the assumed value of T_{if}^* and the calculated value of T_p^* do not agree within allowable tolerance at each point of the product surface, other values of T_{if}^* as determined by the iteration scheme are assumed and the calculations repeated till the assumed value of T_{if}^* and the calculated value of T_p^* agree at every point. The iteration scheme by which the correct values of T_{if}^* are obtained in about five iterations is described hereunder.

Figure 2 gives a schematic representation of the iteration scheme. DEF represents the relation between the assumed value T_A and the calculated value T_C of the temperature at the product–liquid interface. Two arbitrary values of T_A, say T_{A1} and T_{A2} are assumed and the corresponding values of T_{C1} and T_{C2} are obtained after solving the governing equations for the liquid film and the product. The points (T_{A1}, T_{C1}) and (T_{A2}, T_{C2}) are represented by D and F. OB represents the line, $T_C = T_A$. OB and DF (or DF produced) intersect at G. The value of T_A at G, say T_{A3} is used to calculate a third value of T_C say T_{C3}. The point (T_{A3}, T_{C3}) is represented by H. I is obtained by proceeding from H parallel to DF. Using the value of T_A at I, point J is obtained. Iterations are proceeded likewise till point E, where $T_A = T_C$ is reached. Here convergence is ensured even if the initial guess values of T_{A1} and T_{A2} are far away from the converged value.

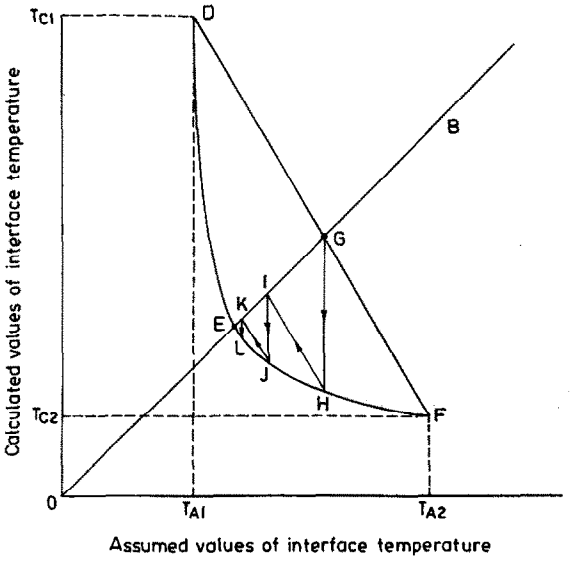

FIG. 2. Schematic representation of iteration scheme.

RESULTS AND DISCUSSIONS

The results are computed for the following governing parameters:

(i) The dimensionless wet bulb temperature of air, T_a^+ is varied from 0.04 to 0.2 in increments of 0.04. This corresponds to a wet bulb temperature range of 2–10°C.

(ii) The dimensionless initial water temperature, T_{f0}^+, is varied from 0.1 to 0.4 in increments of 0.1. This corresponds to a temperature range of 5–20°C.

(iii) Bi is varied from 0.1 to 10.0 as 0.1, 5.0 and 10.0. This range of Bi values covers air velocities up to 5 m/s characteristic dimension of the product up to 20 cm and thermal properties of a wide variety of products.

(iv) The film Reynolds number, Re_m is varied from 0.1 to 1000 as 0.1, 1.0, 10.0, 100 and 1000. This corresponds to a film thickness range of 0.04 to 0.9 mm (over the surface at $\phi = 90°$).

The above ranges of parameters cover the processing conditions, product sizes and thermophysical properties normally encountered in precooling practice. As the main emphasis in the analysis is on the effect of process parameters, the product dependent parameters such as T_{p0}^+, k^*, α^* and R^* are given representative values during computation.

For the above values of variables, analytical results are obtained in terms of dimensionless temperature within the product against dimensionless time parameter. The analysis also yields the temperature profile across the product sections.

Figure 3 shows typical temperature profile within the product at different times prevailing along a diameter at two different values of θ. As is expected, the profiles are symmetrical with respect to the centre for $\theta = 90°$. For $\theta = 30°$, the temperature at $d^* = 0$, which is a point near the bottom surface, comes down with time whereas at $d^* = 1$, a point near the top surface, all profiles approach one temperature which is the initial temperature of water with which the top surface is always in contact.

Figure 4 shows the effect of variation of Re_m at a low value of T_a^+. At the chosen values of other parameters, there is no effect of Re_m for its values greater than 10. Also, for $Re_m > 1$, the final temperature of the product at the centre approaches the initial water temperature, indicated by R_T. $Re_m < 10$ results in a higher product temperature in the beginning of the cooling process than for $Re_m \geq 10$. This is because, in the beginning of cooling, higher heat flux from the product produces a higher interface temperature than T_{f0} due to the insufficiency of film flow for carrying away all the heat. However, at the later stages of cooling, the interaction of air with water film helps to reduce the film temperature in the case of low Re_m.

The effect of varying Re_m at a high value of T_a^+ is given in Fig. 5. This condition represents smaller temperature difference between water and air. Here also, the trend in cooling characteristics is similar to that in Fig. 4. Cooling with low Re_m is slower because

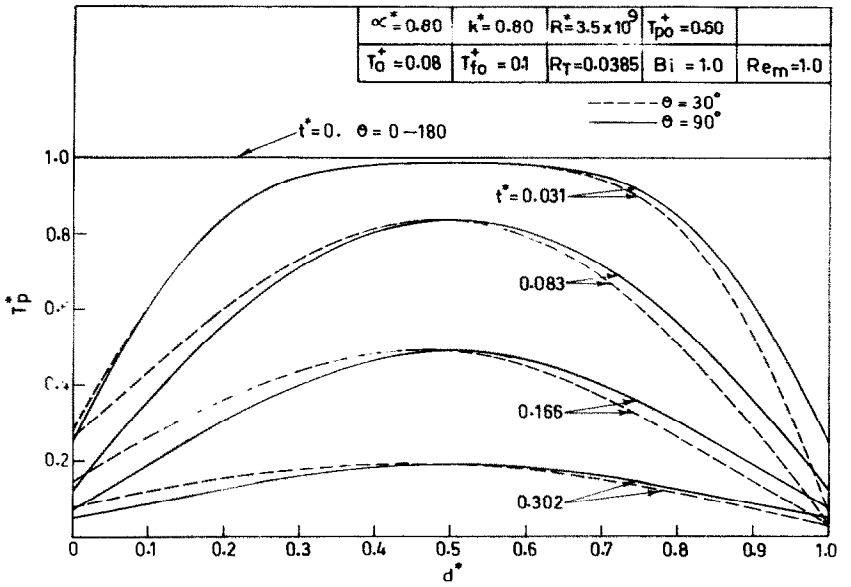

FIG. 3. Typical temperature profile within product.

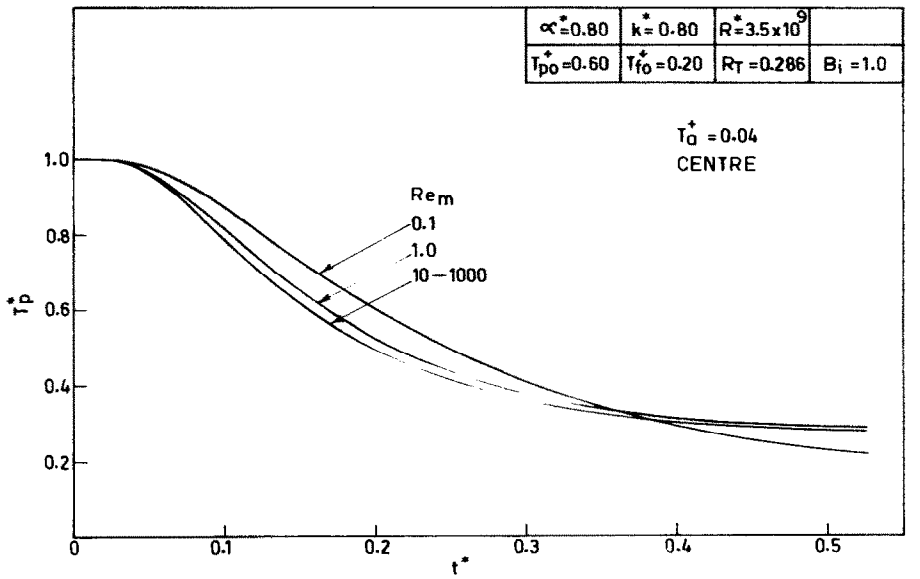

FIG. 4. Effect of film Reynolds number at low T_a^+.

of low interaction between air and water due to low value of *Bi*.

Figure 6 shows the effect of varying Re_m at a low value of *Bi*. It is found that the cooling rate increases with Re_m up to a value of $Re_m = 10$, beyond which the influence of Re_m is negligible. The increase in cooling rate with Re_m is due to the condition of low *Bi* considered here which stipulates a low heat-transfer coefficient. Hence the contribution of air in the cooling process is not significant and cooling rate is mainly dependent on the liquid flow rate which increases with Re_m.

The effect of varying Re_m at a high value of *Bi* is presented in Fig. 7. It may be seen that the trend in cooling characteristics is reversed in this case compared to that at low value of *Bi*. Due to the high *Bi* considered, the influence of air will be felt in the cooling of the film significantly at lower values of Re_m.

In Fig. 8 is given the effect of variation of *Bi* at two different values of T^+_{fo}. It may be seen that for values of other parameters considered, variation of *Bi* over a wide range produces very little effect on the cooling characteristics for $T^+_{fo} = 0.1$ whereas for $T^+_{fo} = 0.4$, the influence of *Bi* is significant. This is because, in the latter case, the temperature difference between water and air is high which results in high heat-transfer

potential. This produces greater cooling at higher *Bi* values. However, it may be seen that smaller difference between air and water produces faster cooling rates.

The effect of *Bi* variation at a low and a high value of Re_m is shown in Fig. 9. As may be seen, for $Re_m = 0.1$, there is considerable increase in the rate of cooling as the *Bi* is increased. This is due to the fact that at high *Bi*, there is more effective interaction of air and water, resulting in the fast reduction in the film temperature which approaches the air temperature represented by '0' on the T_p^* scale. At very high Re_m, variation of *Bi* over wide range has only small influence on cooling because of the high flow rate associated with high Re_m.

Effect of parameters such as T_{p0}^+, k^*, α^* and R^* have also been studied by varying them over wide ranges for fixed values of other parameters. It is observed that only negligible effect on the cooling characteristics is produced by these parameters with the exception of T_{p0}^+.

Figure 10 shows the effect of variation of T_{p0}^+ on the cooling characteristics. It may be observed from the figure that change in T_{p0}^+ affects the cooling rates over wide range of *Bi* values. The higher cooling rates accompanying higher T_{p0}^+ are due to a larger tempera-

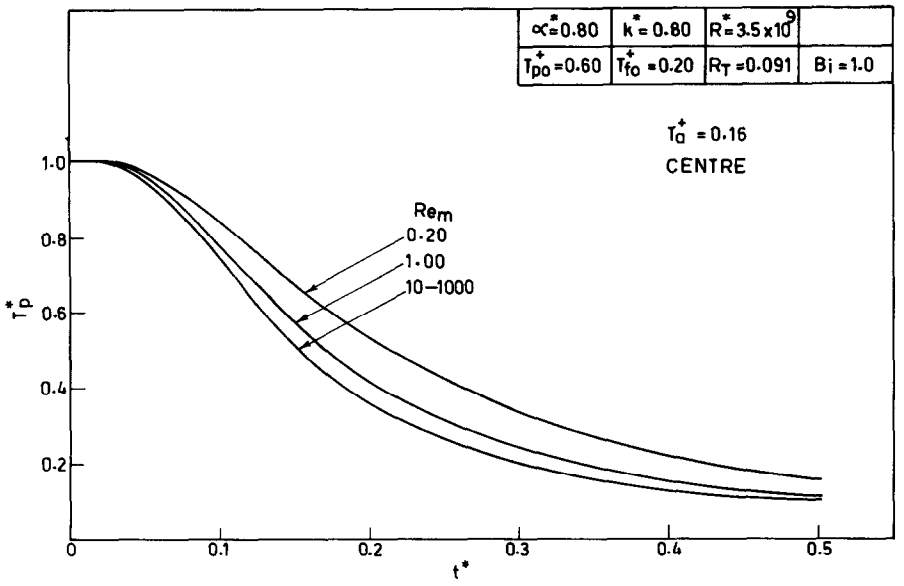

FIG. 5. Effect of film Reynolds number at high T_a^+.

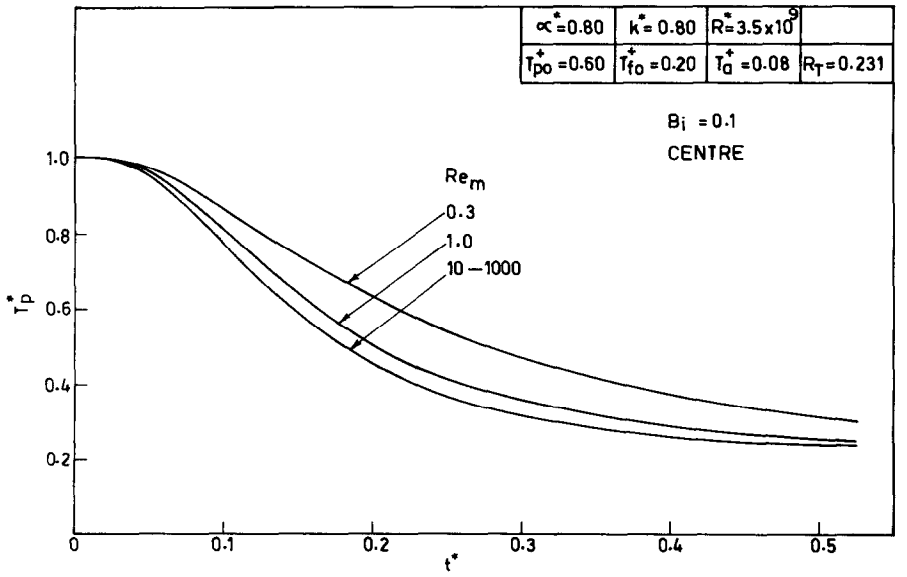

FIG. 6. Effect of film Reynolds number at low *Bi*.

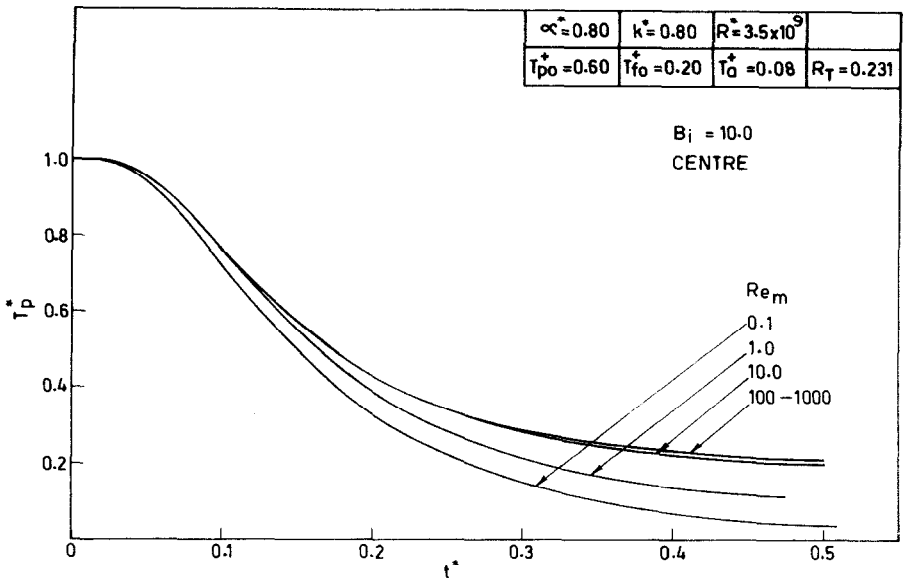

FIG. 7. Effect of film Reynolds number at high *Bi*.

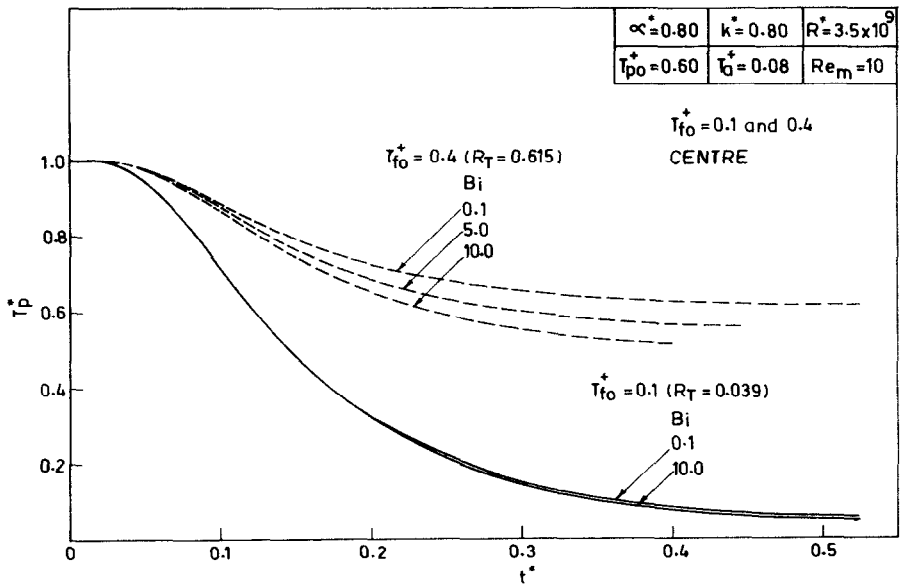

FIG. 8. Effect of Biot number for low and high values of T_{f0}.

ture gradient existing within the product due to the higher initial temperature of the product. However, faster cooling rates here do not necessarily indicate lower product temperatures since T^+_{p0} appear in the definition of T^*_p.

The effectiveness of hydrair cooling can be seen by a comparison with the conventional air cooling. Figure 11 gives the comparison for a typical set of parameters. A low value of 0.1 is used for the film Reynolds number Re_m as hydrair cooling is effective only at low values of Re_m. The figure shows that, at $Bi = 5.0$, air cooling requires 60% more time than hydrair cooling to bring down the temperature to a value of $T^*_p = 0.2$. The difference is less at low value of *Bi*.

It may be seen that hydrair cooling also helps to eliminate dehydration of moist food products which is common with conventional air cooling. The presence of a continuously flowing liquid film over the product surface prevents the formation of a vapour pressure gradient across the product–liquid interface which is the driving force for moisture transfer.

The foregoing discussions reveal that the major

influencing parameters on the hydrair cooling process are Re_f, Bi, T^+_{p0} and the difference $(\Delta T)_{a,f}$ between the initial temperature of water and the wet-bulb temperature of the air defined by,

$$(\Delta T)_{a,f} = T^+_{f0} - T^+_a. \quad (47)$$

With a view to correlate the factors that affect the cooling, the first half cooling time, $Z_{0.5}$ is taken to indicate the cooling speed. In conventional cooling practice, half-cooling time is a measure of cooling speed. In hydrair cooling, due to the presence of water film over the surface of the product, it is observed that half cooling time does not remain constant throughout the cooling process. However, the first half-cooling time may be taken to compare the rate of cooling under different conditions. Of the variables affecting cooling, it has been shown that, the value of the film Reynolds number, Re_m governs the pattern in which the different parameters affect the cooling rate. Thus, it may be seen that when Re_m is included, the variables become uncorrelatable. Hence, a correlation of the first half-cooling time, $Z_{0.5}$ with $(\Delta T)_{a,f}$, Bi and T^+_{p0} is obtained for different constant values of Re_m. Since hydrair cooling is found to be advantageous only at lower values of Re_m the values chosen for Re_m are 0.2, 0.5 and 1.0. The correlation is obtained by the multiple

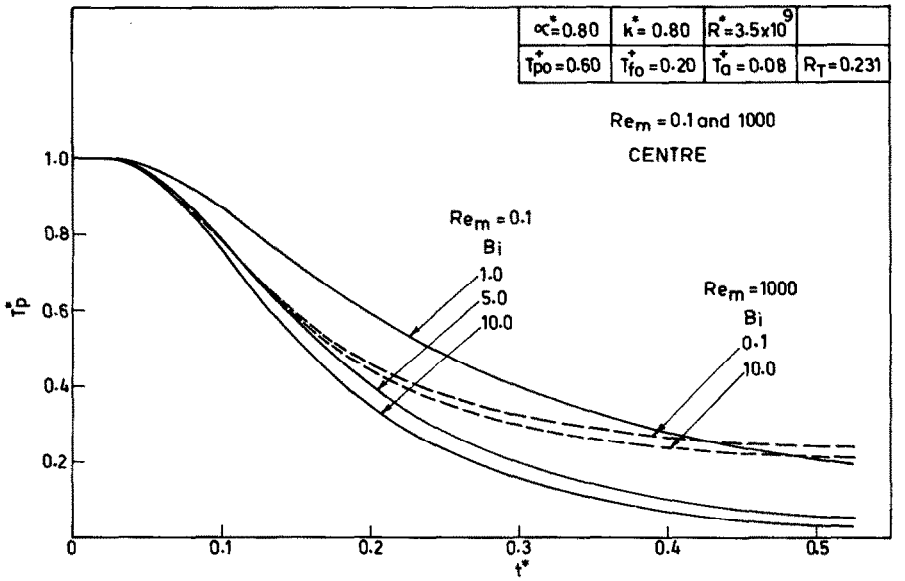

FIG. 9. Effect of Biot number for low and high values of Re_m.

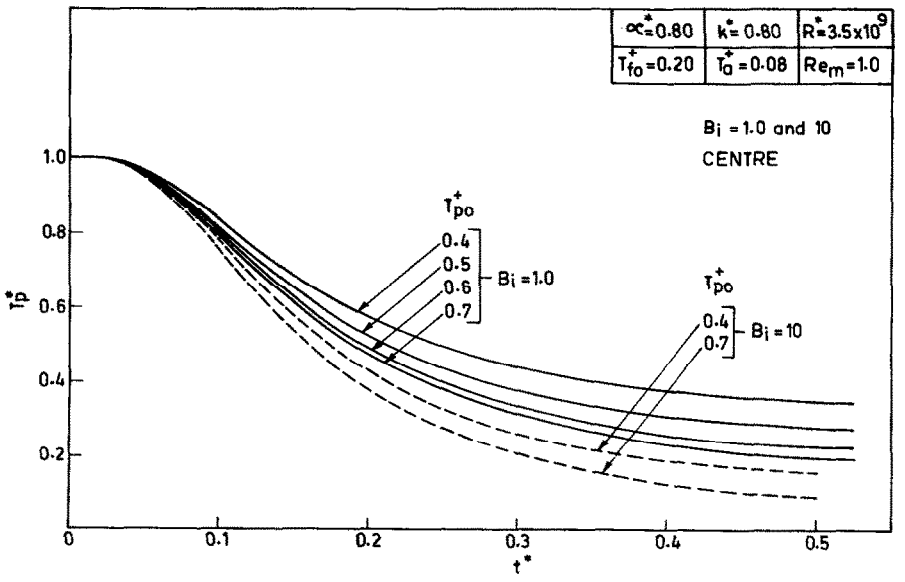

FIG. 10. Effect of initial product temperature.

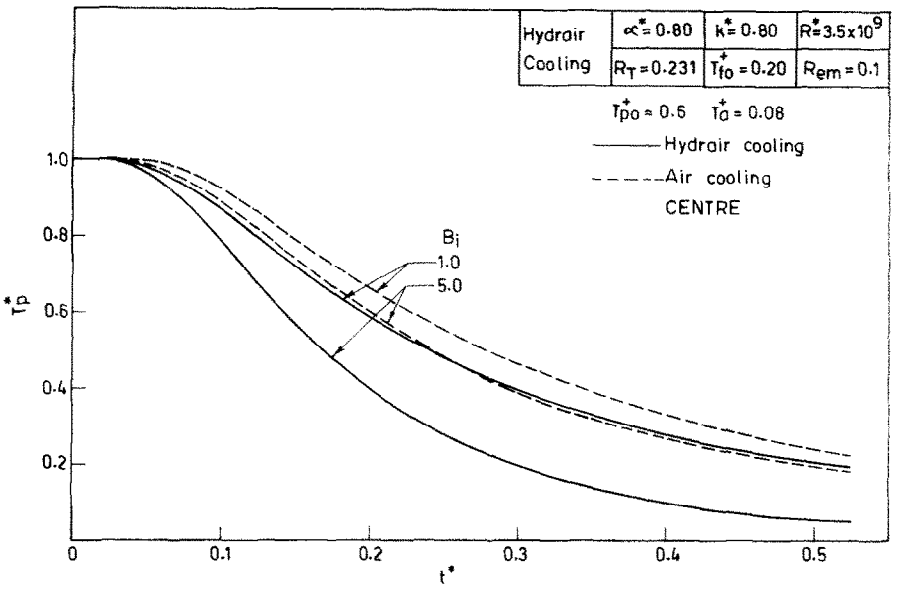

FIG. 11. Comparison with air cooling.

Table 1. $Z_{0.5} = a_1(\Delta T)^{a_2}_{a,f} Bi^{a_3} T^{+a_4}_{p0}$

Product geometry	Re_m	a_1	a_2	a_3	a_4	Correlation coefficient
Sphere	0.2	0.2440	0.0497	− 0.1807	− 0.1066	0.997
	0.5	0.2422	0.0989	− 0.0900	− 0.0980	0.973
	1.0	0.2246	0.1110	− 0.0483	− 0.1526	0.955

linear regression analysis and is of the form:

$$Z_{0.5} = a_1(\Delta T)^{a_2}_{a,f} Bi^{a_3} T^{+a_4}_{p0}. \quad (48)$$

The coefficients a_1, a_2, a_3 and a_4 are given in Table 1.

The correlation covers values of $(\Delta T)_{a,f}$ up to 0.16, Bi up to 5.0, T^+_{p0} from 0.4 to 0.7 and is applicable over wide ranges of α^*, k^* and R^* as it is found that the effect of varying these parameters has negligible influence on cooling.

The correlation can be used for quick estimation of the first half-cooling time of products when the processing conditions and product properties are known. This would also be useful in obtaining an idea about the relative performance of the hydrair cooling process compared to other precooling techniques.

It is to be noted that the analysis presented above is for cooling of a single product. In bulk cooling, the presence of other products can affect the pattern of air flow and film flow past the product. The film flow pattern can still be assumed same as only point contact can theoretically exist between spheres. Hence analysis will hold good for bulk cooling also provided that Biot number is calculated based on the convective heat-transfer coefficient for the air flow conditions prevailing around individual product.

The accuracy of the analytical prediction has been established with the help of elaborate experimentation, the details of which will be presented in a subsequent report.

CONCLUDING REMARKS

An analysis which yields the time temperature histories during hydrair cooling of spherical food products is presented. The cooling speed and the governing parameters are correlated. It has been observed that hydrair cooling process is beneficial at lower values of film Reynolds number, i.e. at lower film flow rates, for smaller differential between air and water temperatures. The cooling effect is pronounced at higher values of Biot number, i.e. at higher air velocities.

REFERENCES

1. F. E. Henry and A. H. Bennett, Hydrair cooling vegetable products in unit loads, *Trans. Am. Soc. Agric. Engrs* **16**(4), 731 (1973).
2. A. H. Bennett and J. M. Wells, Hydrair cooling — a new pre-cooling method with special application for waxed peaches, *J. Am. Soc. Hort. Sci.* **101**(4), 428 (1976).

3. F. H. Henry, A. H. Bennett and K. H. Segall, Hydrair cooling — a new concept for pre-cooling pallet loads of vegetables, *Trans. Am. Soc. Heat. Refrig. Engrs* **82**(2), 541 (1976).
4. P. M. Abdul Majeed, Studies on heat transfer during hydrair cooling of food products, Ph.D. Thesis, Dept. of Mech. Engng, Indian Inst. of Tech., Madras, India (1979).
5. G. D. Fulford, The flow of fluids in thin films, *Adv. Chem. Engng* **5**, 151 (1964).
6. W. F. Stoecker, *Refrigeration and Airconditioning*, p. 252. T.M.H. (1977).
7. *ASHRAE Guide and Data Book (Fundamentals)*. ASHRAE, New York (1971).

ANALYSE DU TRANSFERT THERMIQUE PENDANT LE REFROIDISSEMENT HYDRAIR DE PRODUITS ALIMENTAIRES SPHERIQUES

Résumé — Le refroidissement hydrair des produits alimentaires périssables est envisagé pour allier les avantages du refroidissement à l'air et du refroidissement à l'eau. Cette technique consiste en un passage d'air froid sur un produit qui est continuellement humidifié par un brouillard d'eau pulvérisée. On présente une analyse qui décrit l'histoire temps-température pendant le refroidissement hydrair de produits sphériques. On détermine les domaines des paramètres dans lesquels le mécanisme est les plus efficace. La vitesse de refroidissement est exprimée en fonction des paramètres.

UNTERSUCHUNG DES WÄRMEÜBERGANGS BEI "HYDRAIR-KÜHLUNG" VON KUGELFÖRMIGEN LEBENSMITTELN

Zusammenfassung—Die "Hydrair-Kühlung" von leicht verderblichen Lebensmitteln soll sowohl die Vorteile der Kaltluft- als auch der Eiswasser-Kühlung vereinigen. Das Verfahren besteht darin, kalte Luft über ein Produkt zu leiten, welches kontinuierlich von Eiswasser besprüht wird. Es wird über eine Untersuchung berichtet, in welcher der zeitliche Temperaturverlauf in kugelförmigem Kühlgut während der "Hydrair-Kühlung" ermittelt wurde. Die Parameter-Bereiche, innerhalb deren das Verfahren am effektivsten ist, werden bestimmt. Die Kühlgeschwindigkeit und die bestimmenden Parameter werden miteinander in Beziehung gebracht.

АНАЛИЗ ПЕРЕНОСА ТЕПЛА ПРИ ВОДНО-ВОЗДУШНОМ ОХЛАЖДЕНИИ ПИЩЕВЫХ ПРОДУКТОВ СФЕРИЧЕСКОЙ ФОРМЫ

Аннотация — Водно-воздушное охлаждение пищевых продуктов включает в себя преимущества воздушного и водяного охлаждения. Методика состоит в продувании холодного воздуха над продуктом, непрерывно смачиваемым охлажденной водной аэрозолью. Приведен анализ, позволяющий получить временную зависимость температуры при водно-воздушном охлаждении пищевых продуктов сферической формы. Определены диапазоны параметров, в которых процесс является наиболее эффективным. Получена зависимость между интенсивностью охлаждения и основными параметрами.